Organic LETTERS
Cite This: Org. Lett. XXXX, XXX, XXX−XXX
Letter
pubs.acs.org/OrgLett

A Next Generation Synthesis of BACE1 Inhibitor Verubecestat (MK-8931)

David A. Thaisrivongs,*[,†] William J. Morris,*[,†] Lushi Tan,*[,†] Zhiguo J. Song,[†] Thomas W. Lyons,[†] Jacob H. Waldman,[†] John R. Naber,[†] Wenyong Chen,[†] Lu Chen,[‡] Baoyun Zhang,[‡] and Jun Yang[‡]

[†]Process Research and Development, Merck & Co., Inc., P.O. Box 2000, Rahway, New Jersey 07065, United States
[‡]WuXi AppTec (Shanghai) Pharmaceutical Co. Ltd., 288 Fute Zhong Road, Waigaoqiao Free Trade Zone, Shanghai 200131, China

Supporting Information

ABSTRACT: The development of a commercial manufacturing route to verubecestat (MK-8931) is described, highlights of which include the application of a continuous processing step to outcompete fast proton transfer in a Mannich-type ketimine addition, a copper-catalyzed amidation reaction, and an optimized guanidinylation procedure to form the key iminothiadiazine dioxide core.

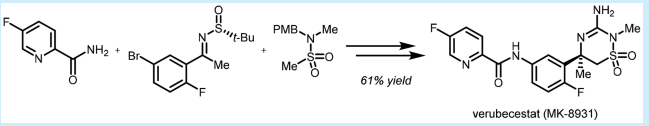

Verubecestat[1] (MK-8931, **1**), currently being evaluated in Phase III clinical trials, is an inhibitor of BACE1 that dramatically reduces the levels of amyloid β peptides in the central nervous system of Alzheimer's disease (AD) patients.[2] Our laboratories have recently disclosed the first generation synthesis of **1**,[3] a route that enabled the discovery, preclinical, and early development research programs. We have also reported a highly efficient second generation synthesis that triples the overall yield of the first.[4] The key features of this latter effort are a diastereoselective Mannich-type addition of a methyl sulfonamide (**3**) to a chiral Ellman sulfinyl ketimine (**2**)[5] to generate the stereogenic tertiary carbamine, a copper-catalyzed C−N coupling of the resultant aryl bromide (**4**) and 4-fluoropicolinamide (**5**), and a late-stage guanidinylation of the penultimate intermediate (**7**) with cyanogen bromide (Scheme 1). The conciseness of this improved synthesis, supported by a minimization of functional group manipulations and protecting group chemistry, provides access to **1** at half the cost of the first generation route and with a more than 70% reduction in the waste generated as judged by the process mass intensity (PMI).[6]

The revised synthesis was successfully executed at scale to support activities related to the verubecestat (**1**) late development program. Nonetheless, several chemical transformations drew our attention as steps that should be able to be conducted with even greater synthetic efficiency. The first was the Mannich-type addition of the lithium anion of **3** to ketimine **2**. Only a moderate assay yield of **4** is obtained at pilot plant scale (70−75%), and the reaction must be performed under cryogenic operating conditions (less than −65 °C), a temperature that not only is highly energy-intensive to achieve and maintain but also imposes significant constraints on the flexibility of both the siting and vessel selection of commercial product manufacture. We have recently reported deuterium quenching studies of this reaction that revealed the competition between the desired 1,2-addition and deprotonation of the electrophile by both the organometallic nucleophile and the unquenched product, experiments which led us to the discovery of a continuous process for this step that controls the selectivity between the various reaction pathways through mixing characteristics in flow.[7] Not only does operating in a continuous instead of batch mode provide a substantially higher assay yield of the desired product (89−91%), but it relieves the reaction of the cryogenic operating requirement; the optimal process temperature is now only −20 °C (Scheme 2).

Contemporaneous with this discovery, we continued to study the copper-catalyzed amidation reaction between 5-fluoropicolinamide (**5**) and aryl bromide **4**, as it too proceeded in only modest yield (70%) at pilot plant scale (Scheme 1). No

Scheme 1. Second Generation Synthesis of Verubecestat (1)

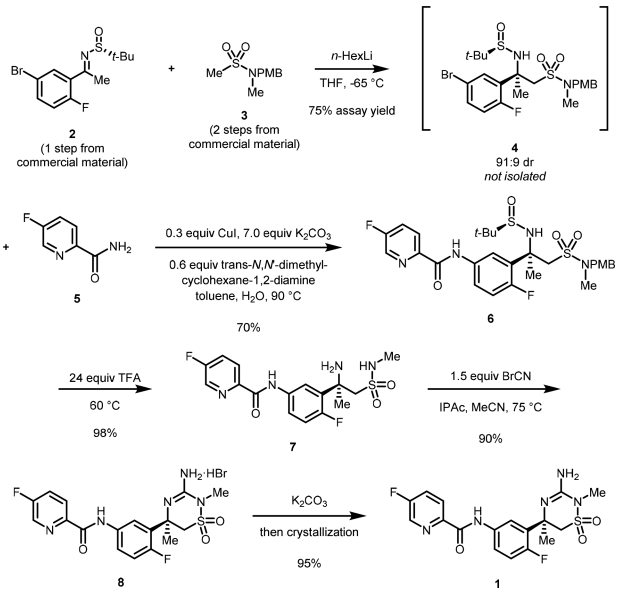

Received: January 28, 2018

© XXXX American Chemical Society

DOI: 10.1021/acs.orglett.8b00259
Org. Lett. XXXX, XXX, XXX−XXX

Scheme 2. Using Flow To Outpace Fast Proton Transfer in the Mannich-Type Addition of 9 to 2

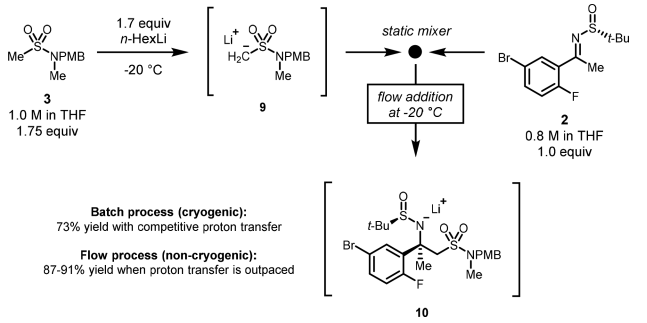

significant improvement was realized through exhaustive high-throughput reaction parameter screening. In considering alternative fragment couplings that might proceed in higher efficiency, we became interested in the reactivity and selectivity of a partially deprotected analog of **5** under similar catalytic conditions. We treated the unquenched product stream from the continuous process (Scheme 2) with excess HCl to selectively and rapidly remove the *N*-*tert*-butanesulfinyl group in the presence of the more acid-stable *para*-methoxybenzyl sulfonamide, which delivered a solution of amine **11** in high assay yield (Scheme 3). Amine **11** is only weakly crystalline, and so the

Scheme 3. Synthesis of Amine 11 and Subsequent C−N Coupling with 5-Fluoropicolinamide (5)

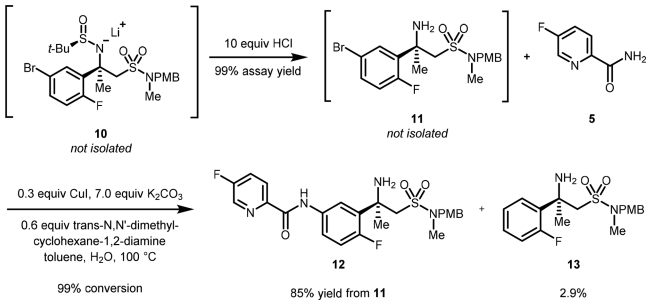

isolation of pure material without resorting to chromatography proved challenging. Nevertheless, we were delighted to discover that, unintuitively, the desired amidation reaction of **11** with **5** proceeded with near-quantitative conversion of the starting material and in higher isolated yield (85%) than the previously employed fully protected aryl bromide **4**. We speculate that **11** could serve as a monodentate ligand for copper, accelerating the aryl amidation reaction by favoring the catalytically active copper−amide species over the unreactive cuprate complex.[8]

trans-*N*,*N*′-Dimethylcyclohexane-1,2-diamine remained the preferred bidentate ligand, as it afforded the best yield while minimizing the amount of ligand-aryl bromide coupled by-product (which we observed with other less sterically hindered diamine ligands such as *N*,*N*′-dimethylethylenediamine and *trans*-1,2,-diaminocyclohexane). Toluene was the optimal solvent to suppress proto-debromination of **11** to amine **13** (Scheme 3). The coupling must be conducted above 100 °C to achieve optimal conversion and avoid significant formation of **13** (Table 1, entries 1 and 2), but diminishing returns were observed at 125 °C (entry 3). Unlike the C−N coupling of the second generation synthesis, only an equimolar amount of ligand was required relative to the copper salt (entry 3), which provides

Table 1. Selected Catalyst Loading and Temperature Optimization Experiments for the C−N Coupling of Aryl Bromide 11 with 5-Fluoropicolinamide (5)

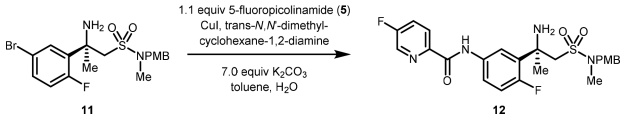

entry	CuI (equiv)	ligand (equiv)	temp (°C)	**13** (%)[a]	conversion (%)[a]
1	0.3	0.6	88	3.0	90.5
2	0.3	0.6	107	1.6	99.3
3	0.3	0.6	125	1.3	99.4
4	0.3	0.3	110	0.6	99.7
5	0.2	0.2	110	0.9	99.5
6	0.1	0.1	110	0.7	92.0

[a]Determined by HPLC analysis.

significant cost-savings at commercial manufacturing scale. This observation was consistent with the hypothesis that the substrate itself can serve to ligate copper, although an exogenous ligand is still necessary to effect this reaction. The decrease in ligand loading also slightly increased the assay yield of **12**, as we found a proportional decrease in the amount of **13** formed (e.g., entries 3 and 4). The catalyst loading can be decreased to only 0.2 equiv with no significant decrease in performance (entry 5), but 0.1 equiv was insufficient for full conversion (entry 6). Under the optimal conditions, **12** was obtained in 90% isolated yield on pilot plant scale.[9]

Together, the novel continuous process for the Mannich-type ketimine addition to prepare **10** and the revised C−N coupling chemistry provided a significant improvement in the overall yield compared to the second generation route. The main challenge to integrating these innovations into a next generation synthesis of verubecestat (**1**) was that, in the previous route, crystallization of intermediate **6** provided the pivotal point of stereochemical purity upgrade (typically from 91:9 dr to >99:1 dr). This isolation was the only stage in the synthesis at which the separation of diastereomers through crystallization was possible, and downstream rejection of the corresponding undesired enantiomers through crystallization was far more modest. Intermediate **4** is a weakly crystalline solid, preventing it from serving as a similar point of diastereomeric control. Thus, we chose to evaluate chiral acid salts of our new C−N coupling precursor **11**, seeking to upgrade the stereochemical purity as early as possible in the synthesis and, critically, to identify an isolable solid intermediate. In high-throughput fashion, we looked for crystalline salts of a wide array of commercially available chiral acids in the presence of **11**; (*S*)-mandelic acid emerged as the most promising.[10] In the optimized crystallization process, the desired salt (**15**) could be isolated in 98.5% yield (relative to the desired enantiomer present in the starting material), 99.9% purity, and 98.8% ee (Scheme 4). Notably, being able to use a water-immiscible solvent such as toluene for the crystallization after an aqueous deprotection of **10** provided a

Scheme 4. Optimized Conditions for the Crystallization of 15

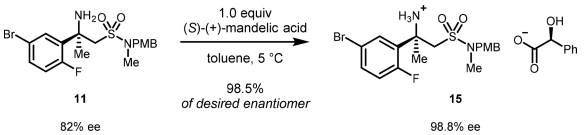

DOI: 10.1021/acs.orglett.8b00259
Org. Lett. XXXX, XXX, XXX−XXX

seamless connection between an organic phase extraction of free-based **11** (the end of the continuous process) and the downstream salt isolation (the starting material for the revised C−N coupling).

With these synthetic improvements in place, we turned to the deprotection of **12**. In the second generation synthesis, the *para*-methoxybenzyl protecting group is removed with neat trifluoroacetic acid (Scheme 1). Faced with the prospect of continuing to use such an excess (24 equiv) of an expensive reagent, we returned to reaction parameter screening in an attempt to uncover a practical and cost-efficient alternative. We overcame the very poor solubility of **7** in most organic solvents by using acetic acid as the bulk media, and although acetic acid was not strong enough to perform the desired transformation efficiently, stronger acids could be added to accelerate the deprotection. Both sulfuric and methanesulfonic acid in the presence of acetic acid provided **7** in equivalently high yield and purity as obtained with the neat trifluoroacetic acid protocol (Scheme 5); we chose to advance the latter acid since sulfuric acid led to intractable emulsions in a variety of aqueous workups.

Scheme 5. Previous Conditions for the Deprotection of 12

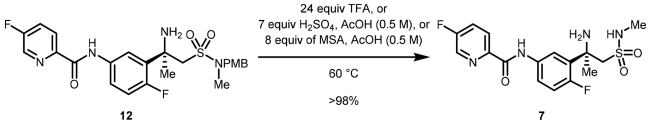

In lab-scale experiments, once the deprotection was complete, the hazy solution was cooled to 20 °C, diluted with water, washed with toluene, and then slowly added to aqueous ammonium hydroxide to effect a pH-driven crystallization of **7**. In our first kilogram-scale batch of the new methanesulfonic acid based procedure, we did not, surprisingly, observe the same hazy solution at the end of reaction. Instead, the solution became clear and the hazy material amassed to a sticky gumball that could not be redispersed into solution with agitation or heat. Analysis of the solid material by MALDI-TOF mass spectrometry revealed many species, the largest of which were over 6000 Da. Each observed peak differed in mass from the others by a multiple of 120 Da (Figure 1), implicating *para*-methoxybenzyl cation polymerization as the source of the gumball. Conducting the deprotection in the presence of 1.0 equiv of the electron-rich arene 1,3-dimethoxybenzene (DMB) completely prevented the formation of higher-order PMB polymers, and the resulting DMB-PMB byproducts were readily removed during the workup in the existing toluene wash (Scheme 6).

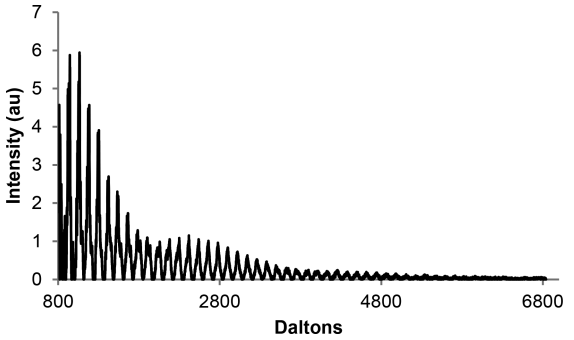

Figure 1. MALDI spectra of PMB polymers from the deprotection of **12** to **7**.

Scheme 6. Optimized Conditions for the Deprotection of 12

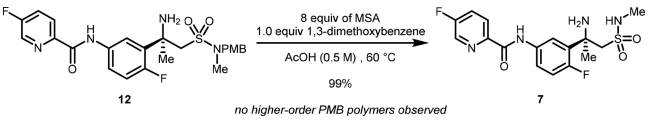

In the second generation synthesis, a reactive crystallization of hydrogen bromide salt **8** provided the basis for an efficient formation of the iminothiadiazine dioxide ring from **7** and cyanogen bromide (Scheme 1). Our laboratories have recently disclosed an unprecedented formation of a 1:1:2 cocrystal of **1**, **7**, and hydrogen bromide, respectively, under these reaction conditions,[11] a singular physical phenomenon that renders the existing process untenable. In renewed efforts to wholly redesign the end game to circumvent this liability, we initially sought to identify basic conditions that would provide a homogeneous reaction and neutralize the problematic hydrogen bromide. In general, we observed low assay yields due to the reaction of **1** (no longer protected as hydrogen bromide salt **8**) with cyanogen bromide. For example, when 0.5 equiv of *N,N*-diisopropylethylamine was used we observed a 8:1 mixture of **1** to overcyanated **16** (Scheme 7).

Scheme 7. Over-cyanation of 1 with Cyanogen Bromide To Form 16 under Basic Reaction Conditions

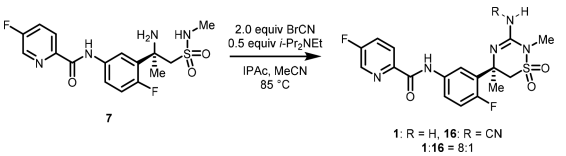

We hypothesized that we could avoid generating either the aforementioned cocrystal or **16** if we developed a process that featured a chemoselective conversion of intermediate **7** to cyanamide **17**, a workup step to remove residual cyanogen bromide, and then a final intramolecular cyclization event to generate **1**. Amine bases weaker than *N,N*-diisopropylethylamine provided cyanamide **17** as the exclusive product, but in only 50−63% conversion (Table 2, entries 1−3). A breakthrough occurred upon the evaluation of inorganic bases, where higher levels of conversion to cyanamide **17** were observed in a range of solvents using either KH_2PO_4 or $NaHCO_3$ (entries 5, 6, 11, and 12). We chose to optimize the reaction with $NaHCO_3$ rather than KH_2PO_4, as the latter presented handling challenges on scale due to its hygroscopicity. When employing $NaHCO_3$, some product decomposition was observed under extended reaction times in MeOH or DMAc (entries 8 and 9). NMP, THF, and 2-MeTHF were differentiated with respect to conversion and stream stability, and similarly high levels of reaction conversion were achieved using 2-MeTHF when the process was conducted at only 45 °C. Following a reductive workup using aqueous sodium thiosulfate to destroy the small amount of residual cyanogen bromide, the 2-MeTHF stream containing cyanamide **17** could be simply treated with aqueous sodium hydroxide to facilitate intramolecular cyclization to **1**, which was accompanied by only trace amounts of overcyanated **16** (Scheme 8). The product was isolated as its *para*-toluenesulfonate salt (**18**) by addition of a solution of *para*-toluenesulfonic acid; a subsequent free-basing with potassium carbonate and crystallization from EtOAc and *n*-heptane provided **1** in 86% isolated yield from **7**.

DOI: 10.1021/acs.orglett.8b00259
Org. Lett. XXXX, XXX, XXX−XXX

Table 2. Selected Optimization Experiments for the Conversion of Amine 7 to *N*-Cyano Intermediate 17

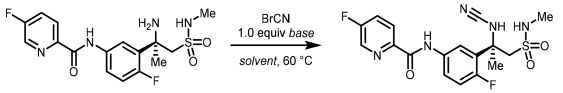

7 17

entry	base	solvent	conversion (%)[a,b]
1	HMDS	MeCN	50
2	diethylaniline	MeCN	56
3	2,6-di-*tert*-butylpyridine	MeCN	63
4	K_2HPO_4	THF	58
5	K_2HPO_4	DMAc	73
6	K_2HPO_4	IPA	86
7	K_2HPO_4	NMP	60
8	$NaHCO_3$	MeOH	63 (54)
9	$NaHCO_3$	DMAc	80 (71)
10	$NaHCO_3$	THF	53 (86)
11	$NaHCO_3$	NMP	96
12	$NaHCO_3$	2-MeTHF	>99[c]

[a]Determined by HPLC analysis after 24 h. [b]Values in parentheses refer to conversion determined after 48 h. [c]Reaction conducted at 45 °C.

Scheme 8. Revised End Game Synthesis of Verubecestat (1)

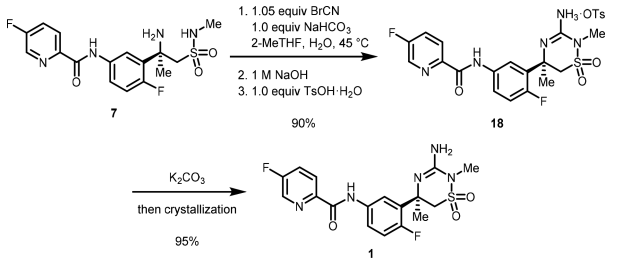

7 18 1

The sum of this work constitutes the third generation synthesis of verubecestat (**1**). The overall yield of 61% from the coupling of **2** and **3** through to **1** improves significantly on the second generation route, for which the same sequence delivers a 44% overall yield. Additionally, gains in efficiency across the overall process produced a further 18% reduction in PMI. These results were enabled by the discovery of a novel continuous process for the Mannich-type ketimine addition used to form the chiral tertiary carbamine, the identification of a new chiral salt (**15**) to provide the key point of stereochemical upgrade, and a new C−N coupling that takes advantage of an unexpected boost in reactivity gained by employing a substrate (**11**) that has been partially deprotected. Further improvements in the end game that enhance the robustness of this process include the use of 1,3-dimethoxybenzene to avoid risks posed by PMB-based polymers in the final deprotection and a new orchestration of the guanidylation sequence to synthesize the iminothiadiazine dioxide ring that circumvents a recently identified cocrystal.

■ ASSOCIATED CONTENT

Supporting Information

The Supporting Information is available free of charge on the ACS Publications website at DOI: 10.1021/acs.orglett.8b00259.

Experimental procedures, compound characterization data, and NMR spectra (PDF)

■ AUTHOR INFORMATION

Corresponding Authors

*E-mail: david.thaisrivongs@merck.com.
*E-mail: william.morris2@merck.com.
*E-mail: lushi_tan@merck.com.

ORCID

David A. Thaisrivongs: 0000-0002-0387-8885
William J. Morris: 0000-0003-4322-4509
Wenyong Chen: 0000-0002-7337-0876

Notes

The authors declare no competing financial interest.

■ ACKNOWLEDGMENTS

We thank Xiaodong Bu, Li Zhang, Erik Regalado, Daniel Zewge, Chunyu Li, and Heather Wang for analytical chemistry support and Becky Ruck, Paul Bulger, and Louis-Charles Campeau for helpful discussions. All are members of Process Research and Development, Merck & Co., Inc.

■ REFERENCES

(1) Scott, J. D.; Stamford, A. W.; Gilbert, E. J.; Cumming, J. N.; Iserloh, U.; Misiaszek, J. A.; Li, G. *PCT Int. Appl.*, WO 2011/044181 A1, PCT/US2010/051553, 2011.

(2) Kennedy, M. E.; Stamford, A. W.; Chen, X.; Cox, K.; Cumming, J. N.; Dockendorf, M. F.; Egan, M.; Ereshefsky, L.; Hodgson, R. A.; Hyde, L. A.; Jhee, S.; Kleijn, H. J.; Kuvelkar, R.; Li, W.; Mattson, B. A.; Mei, H.; Palcza, J.; Scott, J. D.; Tanen, M.; Troyer, M. D.; Tseng, J. L.; Stone, J. A.; Parker, E. M.; Forman, M. S. *Sci. Transl. Med.* **2016**, *8*, 363ra150.

(3) Scott, J. D.; Li, S. W.; Brunskill, A. P. J.; Chen, X.; Cox, K.; Cumming, J. N.; Forman, M.; Gilbert, E. J.; Hodgson, R. A.; Hyde, L. A.; Jiang, Q.; Iserloh, U.; Kazakevich, I.; Kuvelkar, R.; Mei, H.; Meredith, J.; Misiaszek, J.; Orth, P.; Rossiter, L. M.; Slater, M.; Stone, J.; Strickland, C. O.; Voigt, J. H.; Wang, G.; Wang, H.; Wu, Y.; Greenlee, W. J.; Parker, E. M.; Kennedy, M. E.; Stamford, A. W. *J. Med. Chem.* **2016**, *59*, 10435.

(4) Thaisrivongs, D. A.; Miller, S. P.; Molinaro, C.; Chen, Q.; Song, Z. J.; Tan, L.; Chen, L.; Chen, W.; Lekhal, A.; Pulicare, S. K.; Xu, Y. *Org. Lett.* **2016**, *18*, 5780.

(5) (a) Cogan, D. A.; Ellman, J. A. *J. Am. Chem. Soc.* **1999**, *121*, 268. (b) Robak, M. T.; Herbage, M. A.; Ellman, J. A. *Chem. Rev.* **2010**, *110*, 3600.

(6) Jimenez-Gonzalez, C.; Ponder, C. S.; Broxterman, Q. B.; Manley, J. B. *Org. Process Res. Dev.* **2011**, *15*, 912 and references therein.

(7) (a) Thaisrivongs, D. A.; Naber, J. R.; McMullen, J. P. *Org. Process Res. Dev.* **2016**, *20*, 1997. (b) Thaisrivongs, D. A.; Naber, J. R.; Rogus, N. J.; Spencer, G. *Org. Process Res. Dev.* **2018**, 10.1021/acs.oprd.7b00385.

(8) For a report of a similar copper-catalyzed C−N coupling rate enhancement in the presence of *n*-$HexNH_2$, see: Klapars, A.; Huang, X.; Buchwald, S. L. *J. Am. Chem. Soc.* **2002**, *124*, 7421.

(9) See Supporting Information for details on how the Design of Experiments method was used to further optimize this transformation.

(10) See Supporting Information for details.

(11) Artino, L.; Varsolona, R.; Brunskill, A.; Morris, W. J.; Thaisrivongs, D. A.; Waldman, J.; Lyons, T. W.; Xu, Y. *Org. Process Res. Dev.* **2018**, 10.1021/acs.oprd.8b00015.

DOI: 10.1021/acs.orglett.8b00259
Org. Lett. XXXX, XXX, XXX−XXX